The sensitivity of velocities with elevation change

John C. Bancroft

ABSTRACT

Elevation and near surface structure distort a time section. These distortions are reduced by estimating the corresponding travel times to a datum (statics) which are then applied to the time section. If these corrections are small enough, they have a negligible effect on the final processed image. If the static corrections are too large, the assumptions for velocity analysis and migration are violated and incorrect velocities may be estimated. These estimated velocities may not represent the structure of the subsurface. If the statics are "reasonable" then the estimated velocities may allow accurate imaging.

The influence statics on RMS velocities that are used for moveout correction and migration are evaluated with the intent of understanding the results of an estimated velocity structure. Displays show the effect of the elevation change and the total static change on the velocity.

INTRODUCTION

Hyperbolic equations

The root-mean squared (RMS) velocity V_{RMS} allows efficient computation of approximate traveltimes in a medium with reasonable structure. The traveltime for moveout correction T_{MO} is computed from the hyperbolic equation

$$T_{MO}^2 = T_0^2 + \frac{4h^2}{V_{RMS}^2}, \tag{1}$$

where T_0 is the vertical zero offset time and h the half source-receiver offset. The traveltime T_{Mig} defines a diffraction shape for zero-offset data, i.e.,

$$T_{Mig}^2 = T_0^2 + \frac{4x^2}{V_{RMS}^2}, \tag{2}$$

where x is offset from the migration point to a colocated source and receiver.

Shifted diffractions

These equation have asymptotes that intersect at the surface where time $t = 0$ and depth $z = 0$. Applying a time shift to the data moves the asymptote away from the surface, invalidating the above equations to represent the data. Consider Fig. 1 which shows a hyperbolic diffraction (thick solid blue line) centered at T_0. A time shift of δt is subtracted from the times along the hyperbola to produce the dashed blue line defined by T_{shift}, which represents the data shifted by a static δt, i.e.,

$$T_{Shift} = \sqrt{T_0^2 + \frac{4x^2}{V_{RMS}^2}} - \delta t \tag{3}$$

A thin blue line defines the true shape of a diffraction with its apex located at $T_0 - \delta t$. This diffraction (thin blue line) will be correctly migrated with V_{RMS}, but data along the dashed blue line will not.

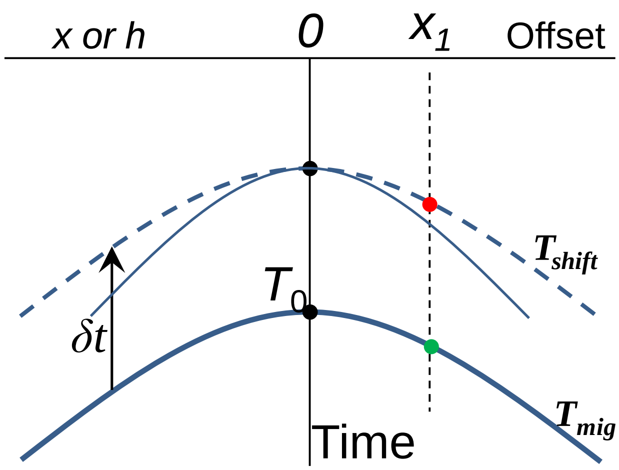

Fig. 1: Illustration of hyperbola and the shifted hyperbola.

Data along the dashed blue line can be approximated by a diffraction in the form of equation (2) by using a different velocity $\boldsymbol{V_{New}}$. We choose to estimate a value for V_{New} by selecting a point at offset $\boldsymbol{x_1}$ on the shifted data as identified by the red dot. The traveltime of a diffraction passing through this point $\boldsymbol{T_{Pnt}}$ becomes

$$T_{Pnt}^2(x_1) = (T_0 - \delta t)^2 + \frac{4x_1^2}{V_{New}^2}, \tag{4}$$

that can then solved for the new velocity,

$$V_{New}^2 = \frac{4x_1^2}{T_{Pnt}^2(x_1) - (T_0 - \delta t)^2}. \tag{5}$$

Substituting equation (3) into equation (5) we have

$$V_{New}^2 = \frac{4x_1^2}{\left(\sqrt{T_0^2 + \frac{4x_1^2}{V_{RMS}^2}} - \delta t\right)^2 - (T_0 - \delta t)^2}, \tag{6}$$

or

$$V_{New}^2 = \frac{4x_1^2}{\frac{4x_1^2}{V_{RMS}^2} - 2\delta t T_0 \sqrt{1 + \frac{4x_1^2}{T_0^2 V_{RMS}^2}} + 2\delta t T_0} . \tag{7}$$

Approximating the square root with the first two terms in its power series we get an approximation

$$V_{New}^2 \approx \frac{4x_1^2}{\frac{4x_1^2}{V_{RMS}^2} - 2\delta t T_0 \left(1 + \frac{2x_1^2}{T_0^2 V_{RMS}^2}\right) + 2\delta t T_0} , \tag{8}$$

which simplifies to

$$V_{New}^2 \approx \frac{V_{RMS}^2}{1 - \frac{\delta t_0}{T_0}} , \tag{9}$$

allowing us to define the new velocity

$$V_{New} \approx V_{RMS} \sqrt{\frac{T_0}{T_0 - \delta t_0}} , \tag{10}$$

which is independent of the choice for x_1. This approximation becomes exact when $x_1 \to 0$ as observed in equation (7), or as derived in the following section. However, equation (7) can still be used to define a best fit diffraction defined at a specific offset.

Equation (10) may also be derived from the curvature of the diffractions at zero offset. The first derivative of equation (2) *wrt x* is

$$2T \frac{dT}{dx} = \frac{8x}{V_{RMS}^2} , \tag{11}$$

or

$$\frac{dT}{dx} = \frac{4x}{T V_{RMS}^2} . \tag{12}$$

Differentiating again *wrt x* gives

$$2T \frac{d^2T}{dx^2} + 2\left(\frac{dT}{dx}\right)^2 = \frac{8}{V_{RMS}^2} , \tag{13}$$

then

$$\frac{d^2T}{dx^2} = \frac{4}{TV_{RMS}^2} - \frac{1}{T}\left(\frac{dT}{dx}\right)^2 . \qquad (14)$$

At the central location of the diffraction, the slope is zero, giving a curvature ***k*** that is proportional to $1/TV^2$. The curvature at $x = 0$ of the shifted and original diffractions is the same, i.e.,

$$TV_{RMS}^2 = \left(T - \delta t\right)V_{New}^2 , \qquad (15)$$

giving

$$V_{New} = V_{RMS}\sqrt{\frac{T}{T - \delta t}} . \qquad (16)$$

This equation defines the velocity of the best fit diffraction at zero offset, and corresponds to the actual definition of the theoretical RMS velocity defined for a medium with constant interval-velocity layers.

Prestack Kirchhoff migrations use similar equations to define the traveltimes from the source to scatterpoint $\boldsymbol{T}_\mathbf{S}$ and the traveltime from the scatterpoint to the receiver $\boldsymbol{T}_\mathbf{R}$ using

$$T_{Mig-\mathrm{Pr}e}^2 = T_S + T_R = \sqrt{\frac{T_0^2}{4} + \frac{h_S^2}{V_{RMS}^2}} + \sqrt{\frac{T_0^2}{4} + \frac{h_R^2}{V_{RMS}^2}} , \qquad (17)$$

where $\boldsymbol{h_S}$ and $\boldsymbol{h_R}$ are the offsets from the migration point to the source and receiver. The asymptotes of these hyperbolas do not intersect at the surface, but a static shift will have the same consequences as the poststack migration case.

The following figure was created to define the new velocity as a function of the change in elevation. Each curve represents a different T_0 on a time section, and they range from 0.4 to 1.5 sec. The red curve represents T_0 = 1.0 sec. The velocity used in this example was 3,000 m/s.

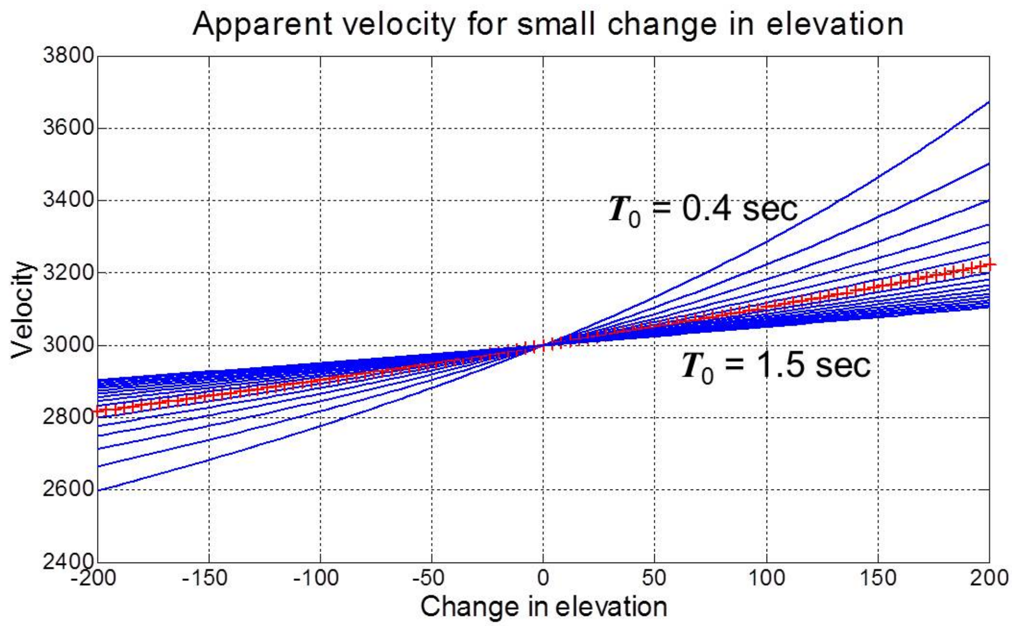

Fig. 2: New velocities plotted as a function of <u>change in elevation</u>. Each curve represent the time T_0 on a time section. The red curve was plotted at T_0 = 1.0 sec.

A plot similar to the elevation static was created to plot the new velocities relative to a defined static shift and is displayed in Fig. 3.

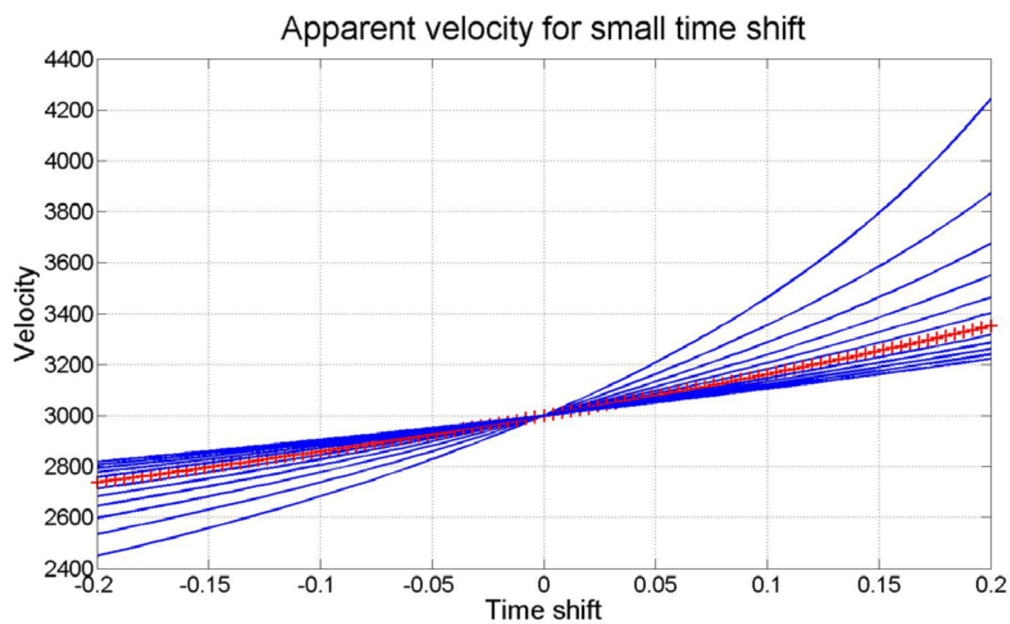

Fig. 3: New velocities (m/s) plotted as a function of <u>change in static</u> (sec.). Each curve represent the time T_0 on a time section. The red curve was plotted to T_0 = 1.0 sec.

.

REAL DATA

A prestack migration using common scatter point (CSP) gathers, forms the gathers without moveout. After they are formed, velocity analysis estimates accurate velocities, then moveout correction completes the prestack migration. These velocities are subject to static shifts. This is evident when data from the Hussar project was processed. The velocity structure was expected to be relatively flat, but that actual velocities picked from the CSP gathers varied considerably. That velocity field is displayed in Fig. 4 and it is conjectured that the varying velocities result from time shifts due to static corrections.

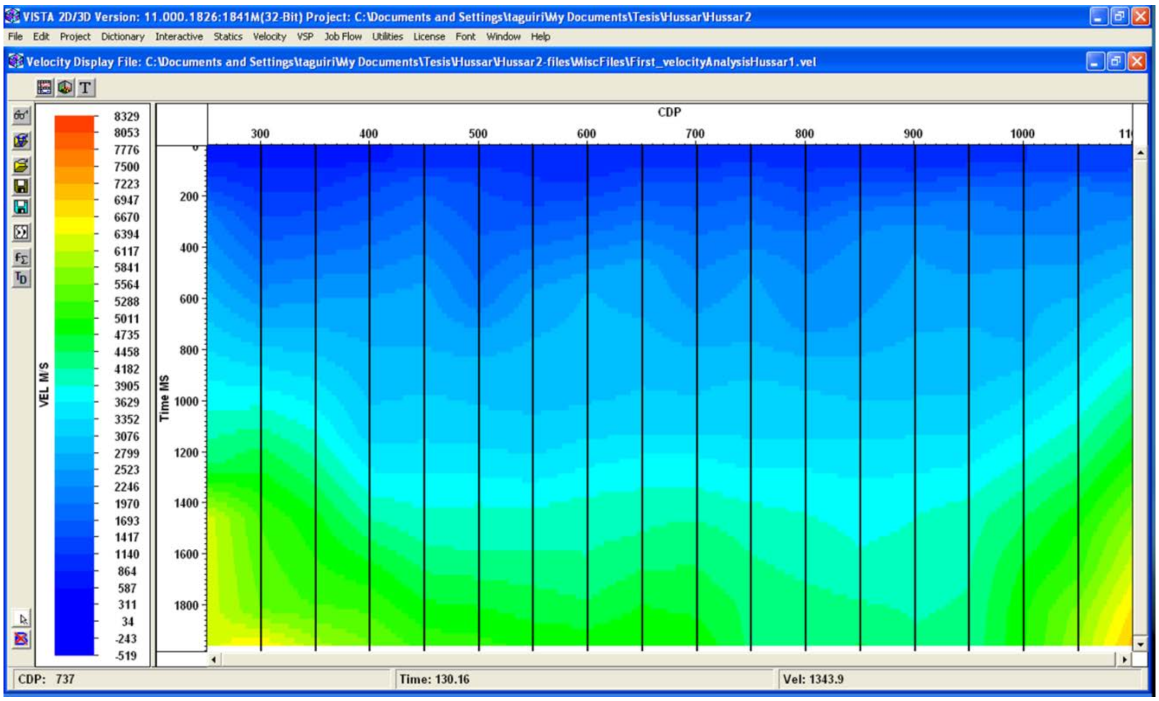

Fig. 4: The velocity field from a Hussar prestack migration using CSP gathers.

The elevation profile for this data is displayed in Fig. 5

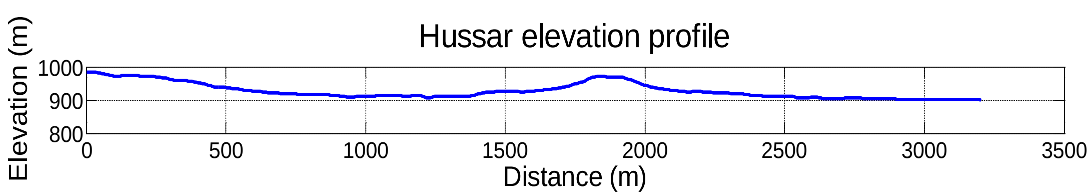

Fig. 5: Elevation profile of the Hussar data.

An example of a CSP prestack migration using the above velocity field is displayed in Fig. 6.

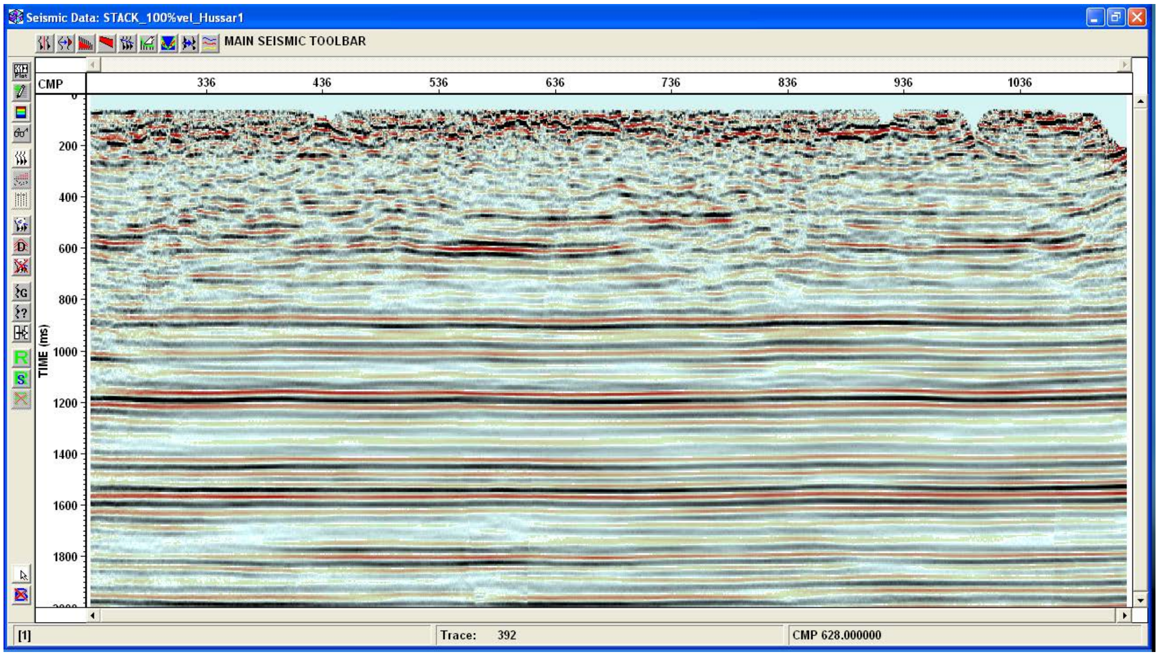

Fig. 6: An example of a prestack migration using CSP gathers, moveout corrected with the velocities displayed in Fig. 4.

COMMENTS AND CONCLUSIONS

Vertical static shifts are used to move data to a processing datum. These shifts modify the velocities required for imaging. These effects were estimated and displayed.

If the static shifts are too large, then imaging assumptions are violated and special processing such as wave-propagation datuming or migration from surface must be used.

ACKNOWLEDGEMENTS

We thank the sponsors of CREWES for their support. We also gratefully acknowledge support from NSERC (Natural Science and Engineering Research Council of Canada) through the grant CRDPJ 379744-08.